Preparation, characterization and catalytic testing over bimetallic Pt-Pd/ HZSM-5 catalysts in NO reduction by propylene

Mounir Sakmeche[1], Elfahem Sakher[2,5], Billel Smili[1,2], Mohamed El amine Dahou[1], Ahmed Belhakem[3], Leila Belgacem[4], Mohammed Messaoudi[6], Samira Benharat[4]*

[1]Laboratory of Catalytic Materials and Industrial Processes (LMPCI)Department of hydrocarbons and renewable energies, Faculty of Science and Technology. University of Adrar, National High way No. 06. Adrar 01000, Algeria.

[2]Department of chemistry, Faculty of Science and Technology, University of Adrar, National High way No. 06. Adrar 01000, Algeria.

[3]Department of Chemistry, University of Mostaganem, B.P 1001, 27000 Mostaganem, Algeria

[4]Research center in industrial technologies CRTI, Cheraga 16014, Algiers, Algeria.

[5]Environmental Research Center (C.R.E), Alzone 23000 Annaba, Algeria.

[6]Department of Biological Sciences, Faculty of Natural and Life Sciences, University of Adrar, Algeria.

E-mail addresses of corresponding author:

mounir.sakmeche@univ-adrar.edu.dz

Abstract:

Bi-functional and bi-metallic ZSM-5 catalysts with different noble metal mass ratios were prepared using the deposition-precipitation method and ionic exchange with NH^{4+}. Systemic XRD, BET/BJH, STEM, and XPS spectroscopy investigations of the structural and electronic properties of these catalysts showed that 2☐3-nm Pt and Pd metallic nanoparticles were highly dispersed over the ZSM-5 support, with strong interactions between Platinum and Palladium, and a good distribution of the acid sites on the surface of the catalysts which have been observed using the FTIR method by adsorption of pyridine. Considering optimized values of NO/C_3H_6 ratio=1 and GHSV= 22000 h^{-1}, some parameters, acidity, temperature, surface morphology, and catalytic activity performance of Pd-Pt/HZSM-5 zeolites were investigated in the selective catalytic reduction of NO by C_3H_6, Pd-Pt/HZSM-5 bi-functional catalysts exhibited improved catalytic properties relative to their monometallic counterparts. The results show that the active components are uniformly dispersed and distribute well in the micro-porous support. For the $Pt_{0.6}Pd_{0.4}$/HZSM-5 catalyst, the maximum conversion of NO to N_2 approached 63% at 450 ºC with 100% N_2 selectivity. By contrast, for the 1%Pt/HZSM-5 catalyst, the maximum NO conversion to N_2 reached 52% at 450 ºC and only 42% for 1%Pt/HZSM-5. The $Pt_{0.6}Pd_{0.4}$/ZSM-5 catalyst also exhibited high durability and catalytic activity at high reaction temperatures.

Key words: *HZSM-5 catalyst, bimetallic Pt-Pd, NO reduction, C_3H_6-SCR, Catalytic activity*

INTRODUCTION

Selective catalytic reduction of NO by hydrocarbons (HC-SCR) under lean burn conditions is a promising way to reduce NO from automobile exhaust and industrial emissions [1, 2]. Among the various catalysts investigated, supported palladium and platinum-based catalysts have shown the highest catalytic activities for NO reduction by Hydrocarbons at temperatures ranging from 200°C to 500°C [3, 4]. However, the high selectivity of N_2O over Pt/Pd-based catalysts limits their applications since N_2O will bring about a severe greenhouse effect. Given the extensive research interest in palladium and platinum catalysts with superior resistance to conversion, these agents have been applied to several reactions, such as CO and hydrocarbon conversion, two significant reactions in automobile exhaust reduction[5]. Several studies have reported that palladium and platinum particles supported with NH_4 ions on different metal oxides (Al_2O_3, TiO_2, SiO_2) effectively mediated C_3H_6-SCR at 200– 500 ºC under excess oxygen[6, 7]. As a representative of solid acid catalysts, ZSM-5 zeolite exhibits firm surface acidity in various catalytic applications[8], especially in high-temperature environments exceeding 500°C, resulting in catalyst deactivation. The functionalization by ion exchange with NH^{4+} ions of the prepared ZSM-5 zeolite and the deposition-precipitation of Pt and Pd metals with low degrees on the internal surface of ZSM-5 can be effectively adjusted to obtain the Pt-Pd/H-ZSM-5 form, which results in increased acidity through the formation of Lewis and Brønsted acid sites, and at the same time the formation of a conserved microporous hierarchical pore structure to improve the conversion capacity and mass transfer of catalysts[9]. Among the catalysts studied, the Pt/ZSM-5 catalyst gave the highest conversion of NO to N_2 but with the formation of N_2O. However, Pd/ZSM-5 catalysts cannot activate hydrocarbons at low temperatures and require improvement under such conditions. Bimetallic catalysts exhibit excellent catalytic performance in the catalytic selectivities of NO reduction due to their unique electronic and geometric properties[10]. However, few previous reports have focused on palladium/platinum-based bimetallic catalysts in the De-NO_x reaction [11, 12].

Moreover, the functionalization by NH_4^+ ions did not significantly affect activity, demonstrating the enhancing effect of alloying H^+ with Pd/Pt. Consequently, the development of other reductants is urgently needed. In this work, we reported that novel Pt/Pd-H/ZSM-5 catalysts have distinct advantages for the selectivity of N_2 and reduction of NO. Therefore, this work uses anhydrous solutions used as sources of Pt and Pd metals to functionalize the HZSM-5 zeolite and compares the monometallic HZSM-5 with the bimetallic HZSM-5 to study the effects of pore structure/texture, the behavior of Pt-Pd metal species, morphology, surface acidity, and NO reduction by SCR-C_3H_6 reaction performance.

EXPERIMENTAL SECTION

Catalyst synthesis

Using sodium aluminate ($NaAlO_2$, Sigma-Aldrich) as the aluminium source and silica gel (SiO_2, Sigma-Aldrich) as the silicon source, the ZSM-5 zeolite with a silicon-aluminium molar ratio of 50 was synthesized by using seed-assisted method (germination method)[13]. After homogenization, we always add a silica gel with adequate tetrapropylammonium hydroxide (TPAOH, Sigma-Aldrich) under vigorous agitation. The gel thus obtained is left to age, without stirring, at room temperature for 24 hours. Then, we bring it to a crystallization temperature varying between 150 °C and 175 °C for a period ranging from 7 days under autogenous

pressure. The solid thus obtained is washed several times with deionized water and calcined at 550° C. for 6 hours. The overall composition of the starting gels is $4.5Na_2O-Al_2O_3-100SiO_2-2880H_2O$ (Si/Al=30 in gel).[9]

The obtained molecular sieve powder was exchanged and stirred in a water bath at 80 °C for 2 h with a solution of NH_4Cl (Sigma Aldrich,1 mol/L) according to the solid-liquid mass ratio of 1:20, the samples were washed and dried at 120°C to evacuate the NH_3, then were calcined at 550°C to obtain molecular sieve sieves of the HZSM-5 form [14, 15].

Metals supported-HZSM-5 catalysts were prepared by the deposition-precipitation (DP) method, using urea as a precipitator. Typically, 1.0 g of ZSM-5 was suspended in an aqueous solution containing anhydrous $PdCl_2$ and $PtCl_2$ at different ratios and urea as the precipitating agent. The solution was heated to 80 °C for 8 h with vigorous stirring, filtered, washed in deionized water, and dried under a vacuum at 25 °C for 12 h. The resulting samples were called Metals/HZSM-5 catalysts [16, 17].

Characterizations

The actual loadings, palladium, and platinum of the catalysts were determined by inductively coupled plasma atomic emission spectroscopy ICP-AES. Powder X-ray diffraction patterns (XRD) were recorded using the test conditions on a Philips PW1830 diffractometer with diffraction source Cu-Kα (λ = 0.15406 nm), 40 kV tube current, 40 *mA*. The BET characterization was done on the ASAP2020 physical adsorption instrument[18]. The study of acidity was done using the FTIR method by adsorption of pyridine (in situ) on the activated catalysts. The values obtained in Table 1 were calculated via the method described in the literature [19], which consists of determining the IMEC (integrated molar extinction coefficients) from the differences in quantities (concentrations) involved in the pyridine that have been adsorbed on the active ingredient acidic sites (Brønsted and Lewis) and the bands of the Py-L and Py-B sites obtained during the analysis with Perkin –Elmer FTIR. The morphology of the samples was taken with a Philips XL series XL 30 FEG, and structures of the metal particles were characterized via scanning on a Merlin Compact scanning electron microscope (HAADF-STEM) operating at 300 KV. X-ray photoelectron spectroscopy (XPS) spectra equipped with a monochromated Al–Ka radiation source (1500 eV) under a residual pressure of 10^{-9} Torr. The measured spectra referenced the graphite C 1s peak at 285 eV[20].

Catalytic test

The catalytic performances of the samples in the Propylene-SCR of NO were measured in a fixed-bed reactor. Before each catalytic test, the catalysts (0.2 g, 20–40 mesh) were reduced in 5% H_2/Ar with a temperature range (100–450 °C) for 8 h and were placed between layers of inert quartz in Q: C: Q: C: Q proportion. The reaction gas comprised V/V of 0.2% NO / 0.2% of C_3H_6 with 4% of O_2 volume at He atmosphere. The total flow corresponds to a space velocity GHSV=22000h^{-1}. The effluent gas was analyzed using an online Agilent 5973 N GC with Porapak Q column (80/100, 2mm ID) coupled to a mass spectrometer (30 m 0.32 mm, 20 mm film) equipped with a TCD, FID, and programmed heating[14]. The selectivity of synthesized catalysts was calculated in terms of the following formulas[21]:

$$NO\ Conversion(\%) = \frac{[NO]in - [NO]out}{[NO]in} \times 100 \quad (1)$$

$$N_2\ Selectivity\ (\%) = \frac{[NO]in - [NO]out - [N2O]out}{[NO]in - [NO]out} \quad (2)$$

RESULTATS AND DISCUSSION

In order to determine the actual platinum and palladium loadings, we used ICP to characterize all the Pt-Pd/HZSM-5 catalysts, as shown in Table 1. The actual platinum and palladium loadings were all lower than the theoretical loadings, attributed to the incomplete precipitation of metallic particles.

Table 1: Structural/textural and acidity characterization of metals/HZSM-5 catalysts

Catalyst	Metals loading (wt %)				Acidity at 450 °C		Acidity at 550°C		Structural proprieties		Pyridine Bands Adsorbed (Cm^{-1})	
	Pt	Pd	Pt	Pd	B	L	B	L	DPA (Å)	S$_{BET}$ (m²/g)	Lewis site	Brønsted Site
HZSM-5	-	-	-	-	16	51	11	5	5.1	365		
Pt / HZSM-5	1	-	0.9	-	18	59	13	8	4.8	331	1591	
Pd / HZSM-5	-	1	-	0.88	19	58	11	7	4.9	338	1570	1544
Pt-Pd/ HZSM-5	0.6	0.4	0.5	0.33	17	62	14	10	4.3	322	1442	

Fig. 1a displays the XRD patterns of the HZSM-5 and Pt-Pd/HZSM-5 catalysts. The diffractogram of Pt-Pd/HZSM-5 after calcination at 823K exhibited peaks at 2theta =7.79°, 8.75°, 23.01°, 23.82° and 24.14° reveals essential intensity peaks indexed as (011), (020), (051), (303) and (313) reflections respectively, which indicates the characteristics of the ordered MFI phase. In the background, Pt-Pd/HZSM-5 diffractogram, different weak peaks attributed to Pt or Pd were observed after impregnation of Platinum at (14.61°, 15.35°, 39.98°) and Palladium at (29.97°, 45.16°) in the HZSM-5 internal surface, which indicated that metals were in the monolithic dispersed in the molecular sieve coating of the catalyst [22].

Fig. 1b shows the results of adsorption/Desorption of N$_2$ and BJH average pore distribution for the HZSM-5 catalyst and support Pt-Pd/HZSM-5. According to the IUPAC classification, nitrogen adsorption isotherms are type I and hysteresis loops were observed at a relative pressure greater than 0.52, due to nitrogen adsorption (intergranular-swelling). The Pt-Pd/HZSM-5 catalyst presents a significantly less intense pore distribution than HZSM-5 and, on the other hand, a maximum pore radius at a slightly lower value. From our BJH results (Table 1), it appears that the decrease in pore diameter for Pt-Pd/ZSM-5 was caused by the exchange with the metals of Pt and Pd, several authors have already observed this phenomenon.
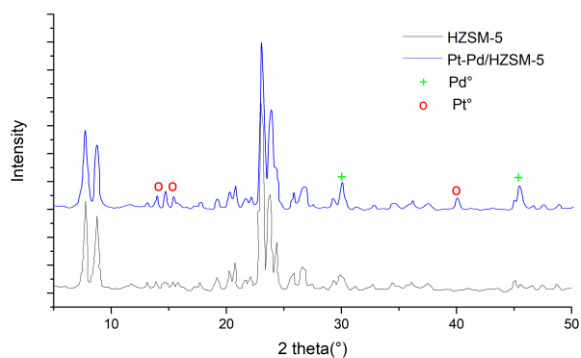
Fig.1a: XRD patterns for the HZSM-5 catalyst and support Pt-Pd/HZSM-5
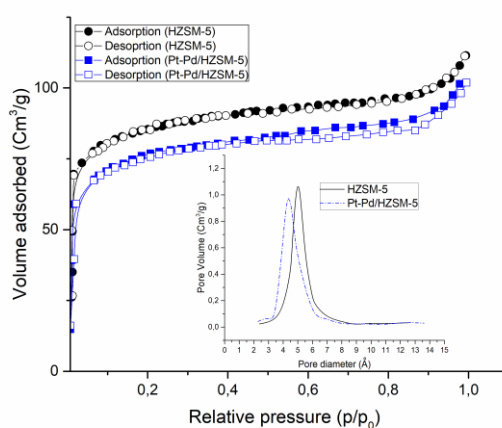

Fig.1b: Adsorption/Desorption of N_2 and BJH average pore distribution for the HZSM-5 catalyst and support Pt-Pd/HZSM-5

A high-angle annular dark field (HAADF-STEM) with an energy-dispersive X-ray spectroscopy (EDX) apparatus was used to analyze the compositions of the platinum and palladium particles. As shown in Fig 2a and 2b, both Pt and Pd signals were detected in freely selected spots, indicating that cloud and different white spots on HAADF-STEM indicate that there is a good distribution of the metals Pt, Pd and the Pd-Pt association on the internal surface of the catalysts and uniform mix of Pt and Pd elements within the particles in the Pt-Pd/HZSM-5 catalysts (Fig. 2 C)[23].

The line scan spectra also show frequency % corresponding to Pt and Pd elements, indicating their presence in the particles. The intensity of the peaks suggests that both elements are present in relatively equal quantities, with the size of selected metallic particles 1 and 2 for the EDX line scan being approximately 2□3 nm, further supporting the formation of a Pt-Pd alloy[24].

The homogeneous dispersion of the metal elements on the catalyst surface is crucial for their effective catalytic performance. The formation of a Pt-Pd alloy enhances the catalytic activity and selectivity of the catalyst compared to individual Pt or Pd nanoparticles. This is because the alloying of Pt and Pd promotes synergistic effects, such as improved stability, enhanced catalytic activity, and increased resistance to catalyst poisoning[25].

Overall, the HAADF-STEM image and EDX line scan spectra provide strong evidence for Pt and Pd's homogeneous dispersion and alloy formation on the Pt-Pd/HZSM-5 catalyst, indicating the potential for high-performance catalytic applications[26, 27].
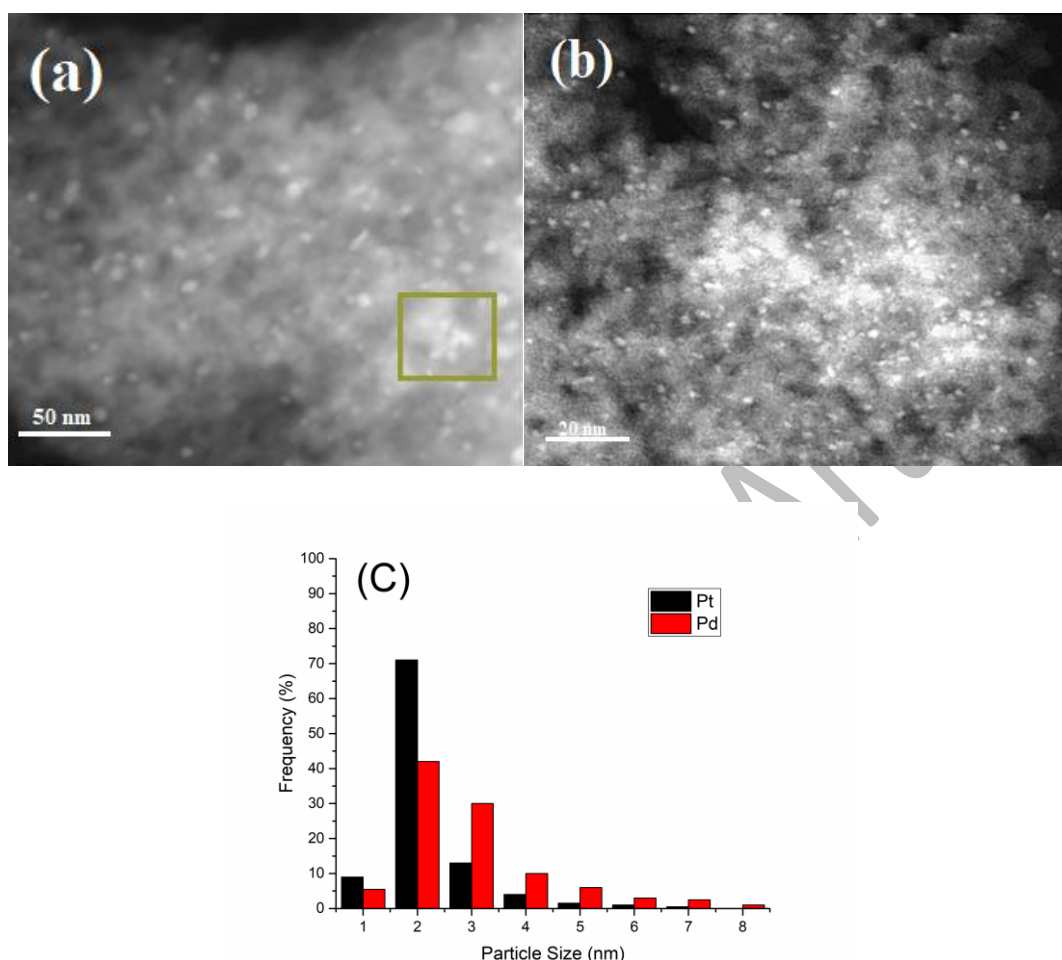

Fig.2: *Metals particles dispersion images and size distribution of Pt0.6Pd0.4/HZSM-5 provided by HAADF-STEM*

The electronic properties of the platinum and palladium particles were analyzed using XPS (Fig 3a,b). As demonstrated in Fig (XPS), the experimental peaks at binding energies of 335.9 - 341.2 eV corresponded with the $3d_{5/2}$ and $3d_{3/2}$ orbital of the Pd^0 species, however, the Pd^0 $3d_{5/2}$ peak in the Pd-Pt/HZSM-5 catalyst experienced a negative shift of 0.3eV and the intensities of these peaks are more critical than observed for, PdOH and PdO species which observed at 342.4 eV and 341.5 eV respectively (Fig 3a)[25, 28, 29].

Unlike palladium, platinum does not readily form oxides that can affect its catalytic power. Platinum is known for its stability and resistance to oxidation because it primarily exists in its metallic forms Pt^0, Pt^{2+}, and Pt^{4+} at 73.8 eV, 74.4 eV, and 75.2 eV, respectively), making it suitable for various catalytic applications (Fig 3b)[30, 31].
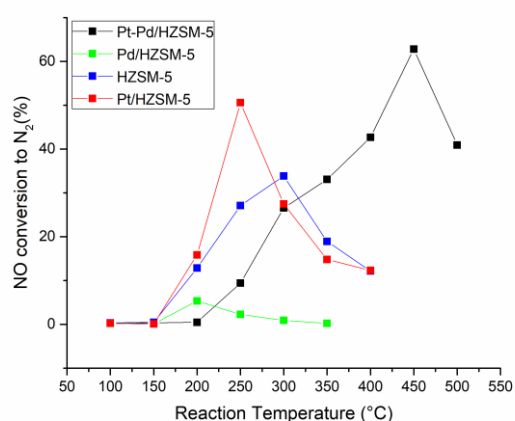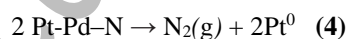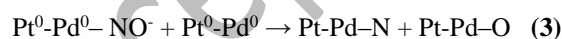
An interaction between Pt and Pd was indicated by a shift in the peaks attributed to the 3d orbital of Pd^0 species 4f orbital of Pt^0 in the bimetallic catalysts to lower binding energies relative to the bi-metallic catalyst. In addition, the position shift of Pd^0 $3d_{5/2}$ decreased as the Pd content increased in the Pt-Pd bimetallic system. This

shift in core binding energy to lower energy indicates a strong interaction between Pt and Pd. Moreover, the degree of the binding energy shift could be used to evaluate the strength of this interaction[25, 32, 33].
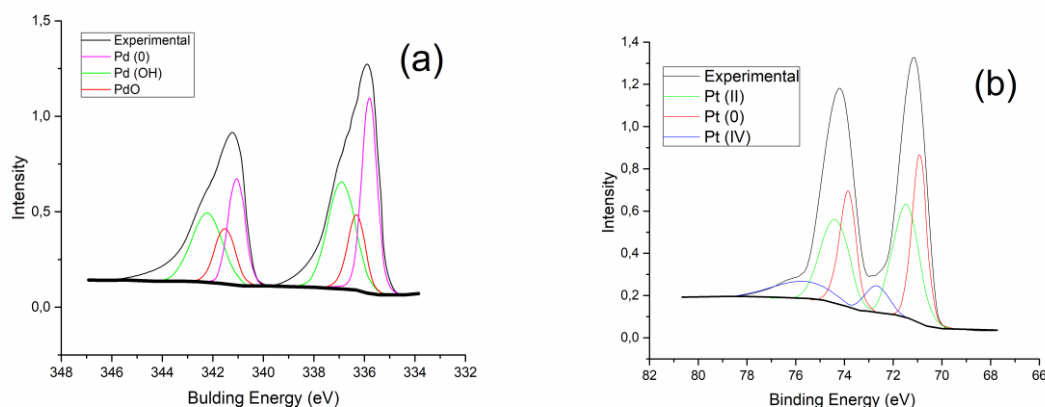
Fig.3: XPS spectra of Pd 3d (a) and Pt 4f (b) of Pt-Pd/HZSM-5 catalysts
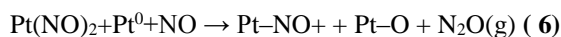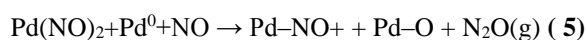
The catalytic activity of metals/HZSM-5 catalyst was assessed in the C_3H_6-SCR of NO in an oxygen-enriched environment. Notably, the Pt-Pd bimetallic catalysts exhibited better catalytic performances regarding Pt/HZSM-5 and Pd/HZSM-5. For instance, the maximum NO conversion to N_2 for the Pt-Pd/HZSM-5 catalyst approached 63% at 450 ºC[34], with 100% N_2 selectivity, implying that the behaviour of Pt-Pd alloy species readily dissociates, producing adsorbed nitride and oxygen atoms according to the reaction mechanism (3,4)[35]. By contrast, the maximum NO conversion to N_2 for the 1%Pt/HZSM-5 catalyst reached 52% and only 42% for 1%Pd/HZSM-5 (Fig.4)[36].

$$Pt^0\text{-}Pd^0\text{–} NO^- + Pt^0\text{-}Pd^0 \rightarrow Pt\text{-}Pd\text{–}N + Pt\text{-}Pd\text{–}O \quad \textbf{(3)}$$

$$2\ Pt\text{-}Pd\text{–}N \rightarrow N_2(g) + 2Pt^0 \quad \textbf{(4)}$$

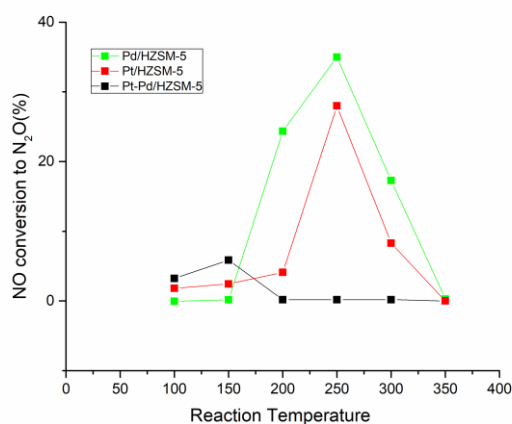*Fig.4: Reaction temperature dependence of NO conversion to N_2 over Different ZSM-5 catalysts*

Moreover, this suggests that the presence of a higher degree of Pd on the catalyst has effects on the catalytic reaction; it lowers the overall temperature required for the side reaction to occur, indicating enhanced catalytic activity, and leads to a slight decrease in the conversion of NO to N_2 due to the formation of N_2O as a secondary

product according to the following reaction mechanism (5,6) [35, 37]. For example, the maximum NO conversion to N_2 was only 5.8% at 150 °C, while the conversion to N_2O at 250 °C reached 28% and 35% for Pt/HZSM-5 and Pd/HZSM-5 respectively (Fig. 5).

$$Pd(NO)_2 + Pd^0 + NO \rightarrow Pd–NO+ + Pd–O + N_2O(g) \quad (\,5)$$

$$Pt(NO)_2 + Pt^0 + NO \rightarrow Pt–NO+ + Pt–O + N_2O(g) \quad (\,6)$$

The results obtained of the performance of propylene conversion versus temperature imply that the behavior of the NO conversion is temperature-dependent. As the temperature decreases, NO conversion is lower, but the formation of N_2O increases[14]. This suggests that optimizing the reaction conditions, including catalyst amount and temperature, is crucial for achieving desired product selectivity in this process. The light-off temperature of propylene oxidation shifted to a lower value as the Pd content increased. For instance, the light-off temperature of propylene oxidation for the Pt-Pd/HZSM-5 catalyst was approximately 100 °C relative to that of the 1%Pd/ZSM-5 catalyst, which was due to the mild promoting effect of Pd (Fig. 6)[38].

Consequently, oxygen vacancies in the Pd-O support are probably to blame for the creation of N_2O on the Pd/HZSM-5 catalyst. On the Pt/ZSM-5, however, a separate process involving dissociative NO adsorption on Pt particles may be in charge of N_2O synthesis. When a bimetallic form is used as a support, the reduced amount of oxygen vacancies present can only partially account for the low N_2O generation. Further research is necessary because additional elements, such as the synergistic action of Pt and Pd, may be necessary [39].
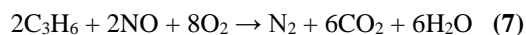

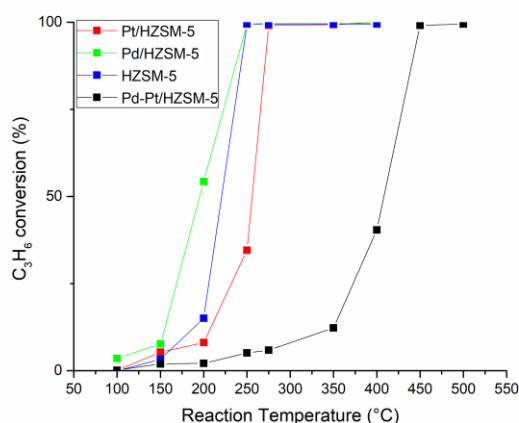*Fig. 5: Reaction temperature dependence of NO conversion to N_2O over Different ZSM-5 catalysts*

On the other hand, this indicates that the presence of the HZSM-5 and Pt/HZSM-5 catalysts has a significant impact on the conversion of C_3H_6 to CO_2 and that the bimetallic Pt-Pd/HZSM-5 catalyst is effective in promoting this catalytic reaction. Additionally, it is observed that the maximum conversions of NO are consistently correlated with the complete conversion of C_3H_6, suggesting that the presence of C_3H_6 plays a crucial role in the NO conversion process. In agreement with our observations, for the Pd/HZSM-5 catalyst, only 5% of NO conversion reacted with C_3H_6 at 270 °C to produce the desired product. This low selectivity suggests that most of the C_3H_6 was being converted to other byproducts or not reacting with NO (Fig. 6)[40].

In summary, the catalytic performances of Pt-Pd bimetallic catalysts were better than those of monometallic catalysts, and this phenomenon was ascribed to the synergistic effect between Pt and Pd. Specifically, Palladium strongly induces hydrocarbon activation at low temperatures, while platinum is highly selective for N_2. In C_3H_6-SCR, adding Pd would thus be expected to promote a propylene partial oxidation reaction and the formation of some reaction intermediates ($C_xH_yO_z$)[41], facilitating the conversion of NO to N_2. It may be involved in the following reaction:

$$2C_3H_6 + 2NO + 8O_2 \rightarrow N_2 + 6CO_2 + 6H_2O \quad \textbf{(7)}$$

$$2C_3H_6 + 9O_2 \rightarrow 6CO_2 + 6H_2O \quad \textbf{(8)}$$

Meanwhile, This suggests that when Pt and Pd are combined in a bimetallic catalyst, their interaction leads to enhanced catalytic activity compared to each metal individually. The presence of Pd in the Pt-Pd catalyst alters the electronic properties of both metals, resulting in a synergistic effect that improves the overall catalytic performance. This implies that the interaction between Pt and Pd in the bimetallic catalyst is crucial for its efficiency and cannot be explained solely by the individual contributions of each metal[42].


Fig. 6: Reaction temperature dependence of C_3H_6 conversion to CO_2 over Different ZSM-5 catalysts

Fig. 7 depicts the stability of the Pt-Pd/HZSM-5 catalyst in the C_3H_6-SCR of NO. The conversion of NO to N_2 was maintained in the range of 60–63% over a 20h period, suggesting that the Pt-Pd/HZSM-5 catalyst was pretty stable[43] due to the presence of Lewis acid sites on bands:1591,1574,1440 cm^{-1} and Brønsted acid sites on band 1544 cm^{-1} in the internal catalyst surfaces and their uniform (Table 1) [19].
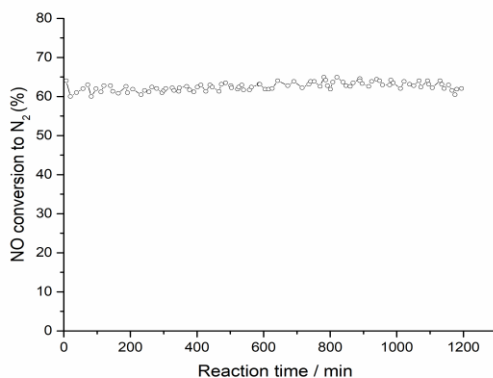
Fig. 7: Dependence of NO conversion to N_2 on reaction time over Pt-Pd/H-ZSM-catalyst at 450°C and GHSV=22,000 h^{-1}.

SEM images indicated that the platinum and palladium particles underwent no apparent changes in size and distribution. Both platinum and palladium particles with sizes of 2–3 nm are highly dispersed over the support. The ICP of platinum and palladium loading for the used catalyst was approximate to the fresh catalyst, proving no significant metals leaching during the reaction process. We attribute the high durability of the Pt-Pd catalyst in the C_3H_6-SCR of NO at 450 ℃ to the good anti-sintering ability of the platinum and palladium particles on the support[18, 44].
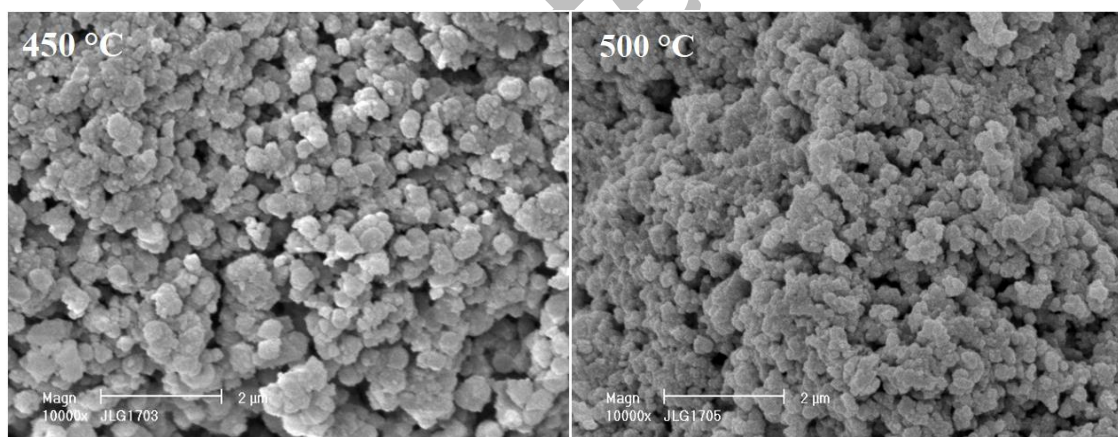
Fig. 8: SEM images of Pt$_{0.6}$Pd$_{0.4}$/HZSM-5 catalysts at 450C$^{•}$ and 500C$^{•}$

The morphologies and structures of the Pt-Pd/HZSM-5catalyst at the optimal temperature of the reaction (450°C) and at 500 °C were characterized by SEM (Fig. 8); the presence of catalysts can significantly affect the particle size and state of aggregation. Catalysts typically provide a surface for the particles to interact and can influence the NO conversion process. However, the catalysts become virtually inactive at elevated temperatures (after 450 °C) [9, 45]. This could be due to the structural collapse of the catalysts and a decrease in the effectiveness of the acid sites Lewis and Brønsted on the catalyst surface (Table 1), to which the corresponding size distribution of the particles is attached.

CONCLUSIONS

The XRD patterns show that the crystallinity of the HZSM-5 catalysts is generally retained, and the structure/texture does not collapse despite the insertion of the low degree of deposition-precipitation Pt and Pd into the internal surface by the deposition-precipitation (DP) method. Significantly, we observed strong interactions between Pt and Pd with sizes of 2–3 nm confirmed by XPS and STEM-EDX in the bimetallic catalysts, which enhanced the excellent catalytic performance of the Pt-Pd/HZSM-5 catalyst. Adding 0.6 wt% Pt and 0.4 wt% Pd promotes the excellent dispersion of metals on the internal surface of HZSM-5, increasing Lewis and Brønsted acid sites. Subsequently, the catalytic performances of these agents in the SCR reduction of NO by C_3H_6 were investigated. The Pd-Pt association on the internal surface of the HZSM-5 catalysts facilitated the activation of propylene at an optimal temperature of 450 °C and improved 63% of the NO conversion to N_2, unlike it is observed that in the Pd/HZSM catalyst -5, the formation of PdO suggests the appearance of 38% of N_2O and secondary products, as well as a remarkable destruction of the catalysts at temperatures that exceed 500C° that leads to a structural collapse and a loss of catalytic activity.

Declaration of conflicting interests

The author(s) declared no potential conflicts of interest concerning this article's research, authorship, and/or publication.

REFERENCES

[1] Mrad R., Aissat A., Cousin R., Courcot D., Siffert S., Catalysts for NOx selective catalytic reduction by hydrocarbons (HC-SCR), Appl Catal A Gen, 504: 542–548 (2015).

[2] Lee K., Choi B., Kim C., Lee C., Oh K., De-NOx characteristics of HC-SCR system employing combined Ag/Al2O3 and CuSn/ZSM-5 catalyst, J Ind Eng Chem, 93: 461–475 (2021).

[3] Fan HY., Shi C., Li XS., Yang XF., Xu Y., Zhu AM., Low-temperature NO x selective reduction by hydrocarbons on H-mordenite catalysts in dielectric barrier discharge plasma, Plasma Chem Plasma Process, 29(1): 43–53 (2009).

[4] Gunnarsson F., Kannisto H., Skoglundh M., Härelind H., Improved low-temperature activity of silver–alumina for lean NOx reduction – Effects of Ag loading and low-level Pt doping, Appl Catal B Environ, 152–153: 218–225 (2014).

[5] Kang SB., Hazlett M., Balakotaiah V., Kalamaras C., Epling W., Effect of Pt:Pd ratio on CO and hydrocarbon oxidation, Appl Catal B Environ, 223: 67–75 (2018).

[6] Captain DK., Amiridis MD., In situ FTIR studies of the selective catalytic reduction of NO by C3H6 over Pt/Al2O3, J Catal, 184(2): 377–389 (1999).

[7] Liu X., Jiang Z., Chen M., Shi J., Zhang Z., Shangguan W., Low-temperature performance of Pt/TiO2 for selective catalytic reduction of low concentration no by C3H6, Ind Eng Chem Res, 50(13): 7866–7873 (2011).

[8]   Zarei T., Davoodbeygi Y., Islamimanesh S., Zarei Z., Methane Dehydroaromatization over Mo and W Catalysts Supported on ZSM-5, Iran J Chem Chem Eng, 41(7): 2278–2287 (2022).

[9]   Smili B., Sakmeche M., Belhakem A., Belgacem L., Tabti C., CO Hydrogenation over functionalized AlMCM-41 materials and ZSM-11/5 zeolites as catalysts, Iran J Catal, 12(3): 337–352 (2022).

[10]   Yang P., Zhou J., Wang Z., Direct decomposition of NO into N2 and O2 over Cu /ZSM-5 containing Ce and Zr as promoter, Adv Mater Res, 113–116: 1735–1739 (2010).

[11]   Liu L., Guan X., Li Z., Zi X., Dai H., He H., Supported bimetallic AuRh/γ-Al2O3 nanocatalyst for the selective catalytic reduction of NO by propylene, Appl Catal B Environ, 90(1–2): 1–9 (2009).

[12]   Panahi PN., Salari D., Niaei A., Mousavi SM., NO reduction over nanostructure M-Cu/ZSM-5 (M: Cr., Mn., Co and Fe) bimetallic catalysts and optimization of catalyst preparation by RSM, J Ind Eng Chem, 19(6): 1793–1799 (2013).

[13]   Nada MH., Larsen SC., Insight into seed-assisted template free synthesis of ZSM-5 zeolites, Microporous Mesoporous Mater, 239: 444–452 (2017).

[14]   Sakmeche M., Belhakem A., Kessas R., Ghomari SA., Effect of parameters on NO reduction by methane in presence of excess O2 and functionalized AlMCM-41 as catalysts, J Taiwan Inst Chem Eng, 80: 333–341 (2017).

[15]   Vessally E., Esrafili MD., Alimadadi Z., Rouhani M., Synthesis of the glycoluril derivatives by the HZSM-5 nanozeolite as a catalyst, Green Chem Lett Rev, 7(2): 119–125 (2014).

[16]   Feyzi M., Lorestani Zinatizadeh AA., Nouri P., Jafari F., Catalytic performance and characterization of promoted K-La/ZSM-5 nanocatalyst for biodiesel production, Iran J Chem Chem Eng, 37(2): 33–44 (2018).

[17]   Babu NS., Lingaiah N., Kumar JV., Prasad PSS., Studies on alumina supported Pd–Fe bimetallic catalysts prepared by deposition–precipitation method for hydrodechlorination of chlorobenzene, Appl Catal A Gen, 367(1–2): 70–76 (2009).

[18]   Sakmeche M., Belhakem A., Ghomari SA., Belgacem L., Hydroconversion of n-C10 alkanes using functionalized AlMCM-41 as catalysts, React Kinet Mech Catal, 129(2): 975–990 (2020).

[19]   Gould NS., Xu B., Quantification of acid site densities on zeolites in the presence of solvents via determination of extinction coefficients of adsorbed pyridine, J Catal, 358: 80–88 (2018).

[20]   Puértolas B., García-Andújar L., García T., Navarro M V., Mitchell S., Pérez-Ramírez J., Bifunctional Cu/H-ZSM-5 zeolite with hierarchical porosity for hydrocarbon abatement under cold-start conditions, Appl Catal B Environ, 154–155: 161–170 (2014).

[21]   Zhang B., Zhang S., Liu B., Shen H., Li L., High N2 selectivity in selective catalytic reduction of NO with NH3 over Mn/Ti-Zr catalysts, RSC Adv, 8(23): 12733–12741 (2018).

[22]   Jesudoss SK., Judith Vijaya J., Kaviyarasu K., John Kennedy L., Jothi Ramalingam R., Al-Lohedan HA., Retraction: Anti-cancer activity of hierarchical ZSM-5 zeolites synthesized from rice-based waste materials, 12: 24139-24139 (2022).

[23]   Chen L., Liang X., Wang D., Yang Z., He CT., Zhao W., et al., Platinum-Ruthenium Single Atom Alloy as a Bifunctional Electrocatalyst toward Methanol and Hydrogen Oxidation Reactions, ACS Appl Mater Interfaces, 14(24): 27814–27822 (2022).

[24]   Lee YW., Ko AR., Han SB., Kim HS., Park KW., Synthesis of octahedral Pt-Pd alloy nanoparticles for improved catalytic activity and stability in methanol electrooxidation, Phys Chem Chem Phys, 13(13): 5569–5572 (2011).

[25]   Wang W., Wang Z., Wang J., Zhong CJ., Liu CJ., Highly Active and Stable Pt–Pd Alloy Catalysts Synthesized by Room-Temperature Electron Reduction for Oxygen Reduction Reaction, Adv Sci, 4(4):1-9 (2017).

[26]   He W., Liu J., Qiao Y., Zou Z., Zhang X., Akins DL., *et al.,* Simple preparation of Pd-Pt nanoalloy catalysts for methanol-tolerant oxygen reduction, J Power Sources, 195(4): 1046–1050 (2010).

[27]   Dong F., Yamazaki K., The Pt-Pd alloy catalyst and enhanced catalytic activity for diesel oxidation, Catal Today, 376: 47–54 (2021).

[28]   Guo Z., Liu T., Li W., Zhang C., Zhang D., Pang Z., Carbon supported oxide-rich Pd-Cu bimetallic electrocatalysts for ethanol electrooxidation in alkaline media enhanced by Cu/CuOx, Catalysts, 6(5):1-14 (2016).

[29]   Thunyaratchatanon C., Luengnaruemitchai A., Jitjamnong J., Chollacoop N., Chen SY., Yoshimura Y., Influence of Alkaline and Alkaline Earth Metal Promoters on the Catalytic Performance of Pd- M /SiO2 (M = Na., Ca., or Ba) Catalysts in the Partial Hydrogenation of Soybean Oil-Derived Biodiesel for Oxidative Stability Improvement, Energy and Fuels, 32(9): 9744–9755 (2018).

[30]   Jiang S., Ma Y., Tao H., Jian G., Wang X., Fan Y., *et al.,* Highly dispersed Pt-Ni nanoparticles on nitrogen-doped carbon nanotubes for application in direct methanol fuel cells, J Nanosci Nanotechnol, 10(6): 3895–3900 (2010).

[31]   Motin AM., Haunold T., Bukhtiyarov A V., Bera A., Rameshan C., Rupprechter G, Surface science approach to Pt/carbon model catalysts: XPS, STM and microreactor studies, Appl Surf Sci, 440: 680–687 (2018).

[32]   Lopes T., Antolini E., Gonzalez ER., Carbon supported Pt-Pd alloy as an ethanol tolerant oxygen reduction electrocatalyst for direct ethanol fuel cells, Int J Hydrogen Energy, 33(20): 5563–5570 (2008).

[33]   Xu J., Ouyang L., Da GJ., Song QQ., Yang XJ., Han YF., Pt promotional effects on Pd-Pt alloy catalysts for hydrogen peroxide synthesis directly from hydrogen and oxygen, J Catal, 285(1): 74–82 (2012).

[34]   Christoforou SC., Efthimiadis EA., Vasalos IA., Catalytic reduction of NO and N_2O to N_2 in the presence of O2., C3H6., SO2., and H2O, Ind Eng Chem Res, 41(9): 2090–2095 (2002).

[35]   Halkides TI., Kondarides DI., Verykios XE., Mechanistic study of the reduction of NO by C3H6 in the presence of oxygen over Rh/TiO2 catalysts, Catal Today, 73(3–4): 213–221 (2002).

[36]   Wen N., Su Y., Deng W., Zhou H., Zhao B., Selective catalytic reduction of NO with C3H6 over CuFe-containing catalysts derived from layered double hydroxides, Fuel, 283 (2021).

[37]   Fuentes CAB., Hwang Y., Catalytic reduction of nitrate in reverse osmosis concentrate by using Pd-Cu/activated carbon felt, Energy Environ, 32(1): 152–167 (2021).

[38]   Imai S., Miura H., Shishido T., Selective catalytic reduction of NO with CO and C3H6 over Rh/NbOPO4, Catal Today, 332: 267–271 (2019).

[39]   Zhou S., Varughese B., Eichhorn B., Jackson G., McIlwrath K., Pt-Cu Core-Shell and Alloy Nanoparticles for Heterogeneous NOx Reduction: Anomalous Stability and Reactivity of a Core-Shell Nanostructure, Angew Chemie, 117(29): 4615–4619 (2005).

[40]   Zhang Z., Chen M., Jiang Z., Shangguan W., Performance and mechanism study for low-temperature SCR of NO with propylene in excess oxygen over Pt/TiO2 catalyst, J Environ Sci, 22(9): 1441–1446 (2010).

[41]   Kalamaras CM., Olympiou GG., Pârvulescu VI., Cojocaru B., Efstathiou AM., Selective catalytic reduction of NO by H2/C3H6 over Pt/Ce1-xZrx2-Δ: The synergy effect studied by transient techniques, Appl Catal B Environ, 206: 308–318 (2017).

[42]   Graham GW., Jen HW., Ezekoye O., Kudla RJ., Chun W., Pan XQ., *et al.,* effect of alloy composition on dispersion stability and catalytic activity for NO oxidation over alumina-supported Pt-Pd catalysts, Catal Letters, 116(1–2): 1–8 (2007).

[43]   Auvray X., Olsson L., Stability and activity of Pd-., Pt- and Pd-Pt catalysts supported on alumina for NO oxidation, Appl Catal B Environ, 168–169: 342–352 (2015).

[44]   Nguyen VT., Nguyen DB., Heo I., Mok YS., Efficient Degradation of Styrene in a Nonthermal Plasma–Catalytic System Over Pd/ZSM-5 Catalyst, Plasma Chem Plasma Process, 40(5): 1207–1220 (2020).

[45]   Ellouh M., Qureshi ZS., Aitani A., Akhtar MN., Jin Y., Koseoglu O., *et al.,* Light Paraffinic Naphtha to BTX Aromatics over Metal-Modified Pt/ZSM-5, ChemistrySelect, 5(44): 13807–13813 (2020).